

Compositional dependence of Raman frequencies in ternary $\text{Ge}_{1-x-y}\text{Si}_x\text{Sn}_y$ alloys

V. R. D'Costa,¹ J. Tolle,² C. D. Poweleit,¹ J. Kouvetakis,² and J. Menéndez¹

¹*Department of Physics, Arizona State University, Tempe, Arizona 85287-1504, USA*

²*Department of Chemistry and Biochemistry, Tempe, Arizona 85287-1604, USA*

(Received 28 March 2007; published 31 July 2007)

The Ge-Ge, Si-Si, and Si-Ge Raman frequencies in $\text{Ge}_{1-x-y}\text{Si}_x\text{Sn}_y$ alloys were measured for $x \leq 0.2$ and $y \leq 0.1$. The Ge-Ge and Si-Si mode frequencies are found to be linear functions of composition over the measured range. The coefficients obtained from linear fits to the experimental data are similar to those measured in binary alloys incorporating Si, Ge, or Sn, suggesting that the linear behavior extends over the entire range of possible compositions (x, y) to include the binary alloys as special cases. The linear coefficients are shown to follow a universal behavior that results from the scaling of phonon dispersion curves in Si, Ge, and α -Sn.

DOI: [10.1103/PhysRevB.76.035211](https://doi.org/10.1103/PhysRevB.76.035211)

PACS number(s): 78.30.Er, 78.20.-e, 61.43.Dg

I. INTRODUCTION

Semiconductor alloys have traditionally attracted great interest as intermediate systems between crystalline compounds and fully disordered amorphous semiconductors. Experimental research has demonstrated that for these alloys it is possible to provide meaningful operational definitions of fundamental quantities that are first introduced in the context of perfectly crystalline semiconductors. These include the lattice constant, band gap, and Raman phonon frequencies, which are found to be smooth functions of the alloy composition. In the simplest case, the compositional dependence reduces to a linear interpolation between the crystalline compounds that are being alloyed. This linear behavior is most commonly found for the lattice constant, as first pointed out by Vegard.¹ In the case of the band gap and the Raman frequencies, deviations from the linear behavior are found in many alloy systems, but—except for a few anomalous cases—the compositional dependence can be quantitatively reproduced by adding a single quadratic term.^{2,3}

Advances in epitaxial growth techniques over the past three decades have made it possible to grow semiconductor heterostructures with defect-free interfaces. Semiconductor alloys play a crucial role in this technology, since—except for a few fortuitous cases—the lattice mismatch between crystalline elemental and compound semiconductors is too large for defect-free growth. In binary A_xB_{1-x} or pseudobinary $A_xB_{1-x}C$ alloys with a one-dimensional compositional space, the composition can be adjusted to match the lattice constant of the substrate, but this leaves no freedom to adjust the band gap of the alloy. The independent adjustment of band gap and lattice constant can be achieved with ternary $A_xB_yC_{1-x-y}$, pseudoternary ($A_xB_yC_{1-x-y}D$), or quaternary ($A_xB_{1-x}C_yD_{1-y}$) materials, and this flexibility explains the great technological interest in two-dimensional alloys. Quaternary systems such as InGaAsSb ,⁴ InGaAsP ,⁵ AlGaAsSb ,⁶ ZnMgSSe , ZnMgBeSe ,⁷ ZnMgSeTe ,⁸ GaInNAs ,⁹ and InGaIn (Ref. 10) are important in optoelectronics. CdMgMnTe has been proposed as a spin injector for spintronic devices.¹¹

The two-dimensional compositional space of ternary, pseudoternary, and quaternary alloys makes it extremely dif-

icult and tedious to map the x, y dependence of the properties of interest. Thus an effort has been under way for many years to understand to what extent this dependence can be predicted from the known compositional dependence of the underlying one-dimensional alloy systems. In a recent paper,¹² we have argued that the recently developed ternary system $\text{Ge}_{1-x-y}\text{Si}_x\text{Sn}_y$ is ideally suited for the investigation of the relationship between “one-dimensional” and “two-dimensional” alloy semiconductors, and we have presented strong evidence that at least some of the interband optical transitions have a compositional dependence that can be explained in terms of the compositional dependence of the same transition in $\text{Ge}_{1-x}\text{Si}_x$, $\text{Ge}_{1-x}\text{Sn}_x$, and $\text{Si}_{1-x}\text{Sn}_x$ alloys. In this paper, we extend this work to the vibrational properties by focusing on the compositional dependence of Raman frequencies in $\text{Ge}_{1-x-y}\text{Si}_x\text{Sn}_y$ alloys.

Earlier studies of the compositional dependence of Raman modes in two-dimensional semiconductor alloys (here, we use the standard language that associates each Raman feature with a vibrational “mode,” although—strictly speaking—alloy disorder causes a continuum of vibrational eigenmodes to become Raman active and contribute to the observed signal) show that random element isodisplacement (REI) models with parameters fit to the underlying one-dimensional alloy systems^{13,14} provide a reasonable explanation of the experimental results. This establishes a correlation between one-dimensional and two-dimensional alloy systems, although the physical validity of the REI models themselves is questionable. For example, REI fits to $\text{Al}_x\text{Ga}_{1-x}\text{As}$ alloys require a 14% change in the cation-anion force constants as a function of composition to explain a $\sim 10\%$ change in Raman peak frequencies over the entire compositional range,¹⁵ whereas first-principles calculations show that the force constants for GaAs, AlAs, and their alloys are virtually identical.¹⁶ Thus REI models may not fully capture the physics of the compositional dependence of phonon frequencies. Ramam and Chua studied the Raman spectrum of $\text{In}_{1-x-y}\text{Ga}_x\text{Al}_y\text{As}$ alloys and concluded that the compositional dependence of the Raman modes in this pseudoternary material *cannot* be expressed in terms of the compositional dependence of the same modes in the three underlying pseudobinary alloys.¹⁷ Polar semiconductors, however, are complicated from this perspective due to the fact that the

compositional dependence of their vibrational modes is determined not only by mass and short-range force perturbations but also by the ionic charges that induce a splitting between longitudinal optic (LO) and transverse optic (TO) modes.³ Therefore, isoelectronic group-IV alloys are, in principle, more attractive for a comparison of the properties of one-dimensional and two-dimensional systems. In addition, the compositional dependence of the Ge-Ge and Si-Si modes is linear for the binary alloys $\text{Ge}_{1-x}\text{Si}_x$ and $\text{Ge}_{1-y}\text{Sn}_y$.^{18,19} Therefore, these modes represent the simplest case to test the correlation between one-dimensional and two-dimensional alloy systems, since for linear dependencies the two-dimensional linear coefficients must be the same as those found in the underlying one-dimensional systems.

The first two-dimensional group-IV alloy whose vibrational properties were studied in detail is the $\text{Ge}_{1-x-y}\text{Si}_x\text{C}_y$ system.²⁰ Unfortunately, carbon-containing alloys are complicated due to the limited solubility of carbon and the possibility that it might occupy interstitial sites in the lattice. Moreover, there is a substantial LO-TO splitting in SiC, and therefore, ionic effects are also expected in ternary group-IV alloys containing C. By contrast, $\text{Ge}_{1-x-y}\text{Si}_x\text{Sn}_y$ alloys represent an ideal test system for a comparative study of the compositional dependence of Raman modes because the amount of Sn that can be substitutionally incorporated in the lattice is much larger, Sn does not occupy interstitial sites, and the ionic effective charges are very small, so that the LO-TO splittings are negligible.

II. EXPERIMENT

A. Sample growth

The $\text{Ge}_{1-x-y}\text{Si}_x\text{Sn}_y$ alloys are grown on $\text{Ge}_{1-y}\text{Sn}_y$ -buffered Si via reactions of SnD_4 and the SiH_3GeH_3 , $(\text{GeH}_3)_2\text{SiH}_2$, $(\text{GeH}_3)_3\text{SiH}$, and $\text{GeH}_3\text{SiH}_2\text{SiH}_2\text{GeH}_3$ hydrides as the sources of the Si and Ge atoms. This class of compounds furnishes building blocks of tailored elemental contents that possess the necessary reactivity to readily form the desired metastable structures and compositions at low temperatures of 300–350 °C. The film growth is conducted by ultrahigh vacuum chemical vapor deposition with a base pressure of 1×10^{-9} Torr. The $\text{Ge}_{1-y}\text{Sn}_y$ buffer layers are grown first on hydrogen-passivated Si(100) wafers at 330–350 °C using well established procedures described previously.²¹ The subsequent growth of $\text{Ge}_{1-x-y}\text{Si}_x\text{Sn}_y$ is conducted *in situ* at reactor deposition pressure of 0.300 Torr, yielding layers with 40–80 nm thickness at a nominal growth rate of ~ 2 nm/min. We produced a host of $\text{Ge}_{1-x-y}\text{Si}_x\text{Sn}_y$ samples with compositions ranging from 13 to 20 at. % Si and from 1.0 to 10.0 at. % Sn. The specific compositions in our experiments were adjusted by varying the concentration of the gaseous reactants in the deposition mixture. Resultant films displayed a mirrorlike appearance similar to that of the underlying Si substrate.

B. Structural characterization

Extensive analyses of the films were carried out to characterize the crystal structure, elemental distribution, and

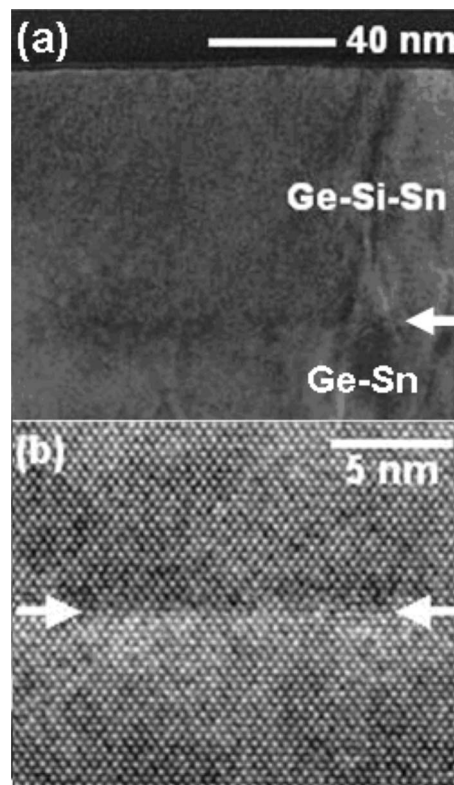


FIG. 1. (a) XTEM diffraction contrast image of $\text{Ge}_{0.98}\text{Sn}_{0.02}/\text{Ge}_{0.72}\text{Si}_{0.18}\text{Sn}_{0.10}$ showing smooth, continuous surface morphology and low defect densities. The arrow marks the location of the interface between the layers. (b) High resolution micrograph of the interface (arrows), indicating perfect epitaxial alignment.

morphological properties by cross sectional transmission electron microscopy (XTEM) (see Fig. 1), electron energy loss nanospectroscopy, Rutherford backscattering (RBS), high resolution x-ray diffraction (XRD), and atomic force microscopy. These techniques collectively demonstrate perfectly epitaxial, uniform, and highly aligned $\text{Ge}_{1-x-y}\text{Si}_x\text{Sn}_y/\text{Ge}_{1-y}\text{Sn}_y$ layers with atomically smooth surfaces and monocrystalline microstructures exhibiting few threading defects. The XTEM data of highly mismatched heterostructures showed that a significant concentration of threading defects originating at the $\text{Ge}_{1-x-y}\text{Si}_x\text{Sn}_y/\text{Ge}_{1-y}\text{Sn}_y$ heterointerface propagates downward and is absorbed by the buffer, thereby yielding in all cases a virtually defect-free epilayer. The RBS studies were particularly useful in determining the atomic compositions (via the RUMP simulation program), the epitaxial registry of the layers, and the phase purity of the samples. The ratio of the channeled vs random RBS peak heights was measured and found to be identical for all constituent elements. This indicates a single-phase material in which the Si, Ge, and Sn atoms occupy random substitutional sites in the same average diamond-cubic lattice as shown in Fig. 2(a) for a $\text{Si}_{0.18}\text{Ge}_{0.75}\text{Sn}_{0.07}/\text{Ge}_{0.97}\text{Sn}_{0.03}$ sample. High resolution XRD (HR-XRD) measurements of the on-axis (004) and asymmetric (224) Bragg reflections were utilized to determine the strain properties of the films. The analyses, in general, reveal that the bilayers adopt strain states which minimize their combined elastic energy, as if the

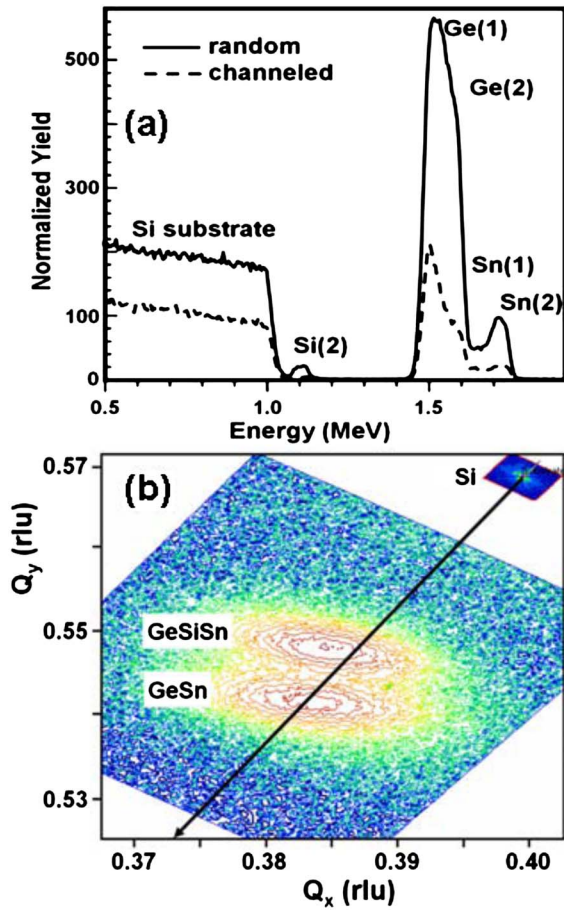


FIG. 2. (Color online) (a) RBS random and channeled spectra of a $\text{Si}_{0.18}\text{Ge}_{0.75}\text{Sn}_{0.07}/\text{Ge}_{0.97}\text{Sn}_{0.03}/\text{Si}(100)$ structure showing the buffer layer and epilayer Si/Ge/Sn peaks labeled as (1) and (2), respectively. (b) Reciprocal space maps showing the (224) reflections of a $\text{Ge}_{0.97}\text{Sn}_{0.03}$ buffer layer and the $\text{Si}_{0.20}\text{Ge}_{0.78}\text{Sn}_{0.02}$ epilayer relative to that of the Si substrate. Note that the relaxation line connecting the Si peak to the plot origin passes near the center of GeSn peak and slightly below the SiGeSn peak, indicating that the buffer is nearly stress-free while the epilayer is tensile strained. The data also indicated that the in plane lattice dimensions of the two layers are virtually identical.

films were decoupled from the substrate. Figure 2(b) shows the (224) reciprocal space maps for a representative $\text{Si}_{0.20}\text{Ge}_{0.78}\text{Sn}_{0.02}/\text{Ge}_{0.97}\text{Sn}_{0.03}/\text{Si}(100)$ sample. These data show that the $\text{Ge}_{1-x-y}\text{Si}_x\text{Sn}_y$ epilayer is highly aligned and tensile strained with respect to $\text{Ge}_{1-y}\text{Sn}_y$ buffer, which possesses a slight compressive strain. In Table I, we show all relevant structural parameters for our ternary alloys, obtained from RBS and x-ray diffraction. The relaxed lattice constant a is computed from the measured a_{\parallel} and a_{\perp} by assuming a tetragonal distortion and using an elastic constant ratio C_{12}/C_{11} that is interpolated between those of Si, Ge, and α -Sn. As seen in Table I, the results are in excellent agreement with a calculation of the ternary lattice constant based on Vegard's law, except at the lowest Sn concentrations, for which the analysis of the RBS data is more complicated due to the similar Sn concentrations in the buffer and the epilayer. It is interesting to note that the deviations from Vegard's law in $\text{Ge}_{1-x}\text{Si}_x$ and $\text{Ge}_{1-y}\text{Si}_y$ alloys are small and of opposite signs,²² so that they might tend to cancel out in the case of the ternary $\text{Ge}_{1-x-y}\text{Si}_x\text{Sn}_y$ alloy.

C. Raman studies

Micro-Raman experiments were performed at room temperature in the backscattering $z(x,y)\bar{z}$ and $z(x,x)\bar{z}$ configurations, where x , y , and z correspond to the 100, 010, and 001 crystal directions, respectively. The light was focused onto the sample with a microscope objective with a magnification of $100\times$. The total laser power was 2.5 mW, and the laser wavelength was 514.5 nm. A single-stage 0.25 m monochromator equipped with a 2400 lines/mm grating and a charge coupled device detector was employed to analyze the scattered light. Figure 3 shows a typical Raman spectrum for a $\text{Ge}_{0.75}\text{Si}_{0.18}\text{Sn}_{0.07}$ alloy. The ternary Raman spectrum is dominated by three peaks, which are assigned to Ge-Ge, Si-Ge, and Si-Si vibrations. No separate Ge-Sn or Si-Sn peaks are observed, although the latter, if present, are likely to be too close to the Si-Ge peak to be observable as a separate feature. This is discussed in more detail below.

The peak positions are extracted from the data following a methodology similar to the one developed by Lockwood and

TABLE I. Summary of structural and Raman data for our samples. Compositions are obtained from RBS, and the lattice constants are obtained from HR-XRD. The relaxed lattice constant is calculated by assuming that the films are under tetragonal distortion and using a linear interpolation of elastic constant ratios. The Vegard lattice constant corresponds to a linear interpolation between Si, Ge, and α -Sn. The Raman frequencies correspond to strain-relaxed films.

x (%)	y (%)	a_{\parallel} (Å)	a_{\perp} (Å)	a (Å)	a_{Vegard} (Å)	$\omega_{\text{Si-Si}}$ (cm^{-1})	$\omega_{\text{Si-Ge}}$ (cm^{-1})	$\omega_{\text{Ge-Ge}}$ (cm^{-1})
0	0	5.6575	5.6575	5.6575	5.6575			301
18	10	5.6620	5.7280	5.7008	5.7000	446.1	389.8	288.8
20	8	5.6779	5.6779	5.6779	5.6787	451.8	393.4	289.9
18	7	5.6730	5.6753	5.6744	5.6750	452.9	394.9	290.9
13	3	5.6761	5.6524	5.6620	5.6530	454.8	395.7	296.7
20	2	5.6654	5.6352	5.6476	5.6288	458.3	400.6	295.6

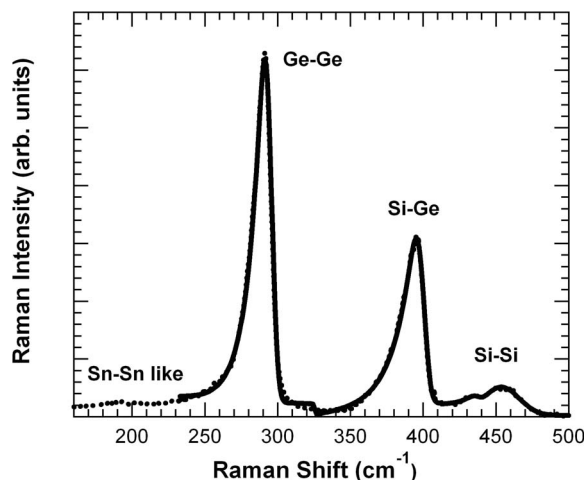


FIG. 3. Room temperature Raman spectrum of a $\text{Ge}_{0.75}\text{Si}_{0.18}\text{Sn}_{0.07}$ alloy obtained in the $z(x,y)\bar{z}$ scattering configuration with $x=(100)$ and $z=(001)$. The excitation wavelength is 514.5 nm. The solid line represents the model fit, from which the peak frequencies were extracted. The peaks associated with Ge-Ge, Si-Si, and Si-Ge vibrations were fitted separately. The peak at 435 cm^{-1} is a well-known feature attributed to isolated pairs of Si atoms.

Wasilewski for $\text{Al}_x\text{Ga}_{1-x}\text{As}$ alloys.²³ The peaks are fitted with an expression of the form $I(\omega) = I_{\text{back}}(\omega) + I_{\text{EMG}}(\omega)$. The background intensity $I_{\text{back}}(\omega)$ is taken as $b_1 + b_2\omega^{-m}$, and the exponentially modified Gaussian (EMG) function $I_{\text{EMG}}(\omega)$ is defined as

$$I_{\text{EMG}}(\omega) = \frac{a}{2s} \exp\left(\frac{w^2}{2s^2} + \frac{\omega_0 - \omega}{s}\right) \times \left[\text{erf}\left(\frac{\omega - \omega_0}{\sqrt{2}w} - \frac{w}{\sqrt{2}s}\right) + \frac{s}{|s|} \right], \quad (1)$$

where a is the peak area, ω_0 the mode frequency, w is the width, and s is the asymmetry parameter. The agreement between model and data is apparent in Fig. 3. The four parameters of the EMG function as well as the parameters b_1 , b_2 , and m from the background function are obtained from the fit. Notice that if the profile is asymmetric, the frequency ω_{max} at which the I_{EMG} function for a single peak has its maximum is *not* equal to the mode frequency parameter ω_0 . We follow the customary approach for alloy semiconductors and use ω_{max} as the peak position to be compared with theory.

Since our alloys possess a small amount of strain, we calculate the strain-induced shifts by assuming a tetragonal distortion, and subtract them from the observed Raman shifts to obtain the Raman frequencies corresponding to relaxed alloys. Phonon strain coefficients for ternary $\text{Ge}_{1-x-y}\text{Si}_x\text{Sn}_y$ alloys have not been measured experimentally, so that we use values for pure Ge or $\text{Ge}_{1-x}\text{Si}_x$ alloys. We take (in cm^{-1}) $\Delta\omega_{\text{Ge-Ge}}^{\text{GeSiSn}}(x,y) = -415\varepsilon_{\parallel}(x,y)$,²⁴ $\Delta\omega_{\text{Si-Ge}}^{\text{GeSiSn}}(x,y) = -575\varepsilon_{\parallel}(x,y)$,²⁵ and $\Delta\omega_{\text{Si-Si}}^{\text{GeSiSn}}(x,y) = -984\varepsilon_{\parallel}(x,y)$.²⁶ Here, ε_{\parallel} is defined as $\varepsilon_{\parallel} = (a_{\parallel} - a)/a$, where a_{\parallel} is the lattice constant in

a direction parallel to the growth plane, and a is the relaxed lattice constant.

III. DISCUSSION

A. Mode identification

The Raman spectrum of our ternary $\text{Ge}_{1-x-y}\text{Si}_x\text{Sn}_y$ alloys is very similar to the Raman spectrum of binary $\text{Ge}_{1-x}\text{Si}_x$ alloys with comparable Ge contents, and therefore, the three dominant structures have been assigned to Ge-Ge, Si-Ge, and Si-Si modes. In the ternary alloy, however, we might expect to see evidence for Sn-Sn, Ge-Sn, and Si-Sn vibrations. The first two have been observed in binary $\text{Ge}_{1-y}\text{Sn}_y$ alloys, although they are weak at the compositions that are experimentally accessible. Evidence for a Raman signal below 200 cm^{-1} , indicative of Sn-Sn vibrations, is also found in our ternary samples. As in the binary alloy, however, the polarization selection rules are unusual [the signal is stronger for the $z(x,x)\bar{z}$ configuration], suggesting that the feature is not entirely opticlike. Therefore we postpone the analysis of this feature until more detailed modeling sheds light on the nature of the vibrations that give rise to the observed Raman activity below 200 cm^{-1} . As to the Ge-Sn mode, we have recently observed it in $\text{Ge}_{1-y}\text{Sn}_y$ alloys excited with 647 nm light, probably because this wavelength is close to resonance with the material's E_1 gap. Unfortunately, the penetration depth of 647 nm in our ternary alloy is long enough to excite the $\text{Ge}_{1-y}\text{Sn}_y$ buffer layer, so that it is very difficult to separate the Ge-Sn signal arising from the buffer layer from a possible Ge-Sn signal originating in the ternary alloy. Furthermore, we believe that the possible presence of a Si-Sn feature is hidden by its close proximity to the Si-Ge modes. Very recently we have confirmed this in measurements of $\text{Si}_{1-y}\text{Sn}_y$ alloys.²⁷ The proximity of the two modes can be understood from the observation that phonon frequencies in group-IV semiconductors scale with the ionic plasma frequency,²⁸ that is, $\omega \propto a^{-3/2}\mu^{-1/2}$, where a is the lattice constant and μ the reduced mass of the unit cell. Since Si is much lighter than Ge or Sn, the reduced mass is close to the Si mass, and therefore, the frequencies of optical Si-Ge and Si-Sn vibrations should be similar. Therefore, the Raman feature near 400 cm^{-1} is probably a mixture of Si-Ge and Si-Sn vibrations, but given the higher number of Si-Ge bonds in our samples and the weakness of the Ge-Sn features in $\text{Ge}_{1-y}\text{Sn}_y$ alloys, we will continue to refer to it as the Si-Ge mode.

B. Compositional dependence of Ge-Ge and Si-Si modes

The Ge-Ge and Si-Si mode frequencies in binary $\text{Ge}_{1-x}\text{Si}_x$ alloys are given by

$$\omega_{\text{Ge-Ge}}^{\text{GeSi}}(x) = \omega_0^{\text{Ge}} - \alpha_{\text{Ge-Ge}}^{\text{GeSi}}x, \quad (2a)$$

$$\omega_{\text{Si-Si}}^{\text{GeSi}}(x) = \omega_0^{\text{Si}} - \alpha_{\text{Si-Si}}^{\text{GeSi}}(1-x), \quad (2b)$$

where $\omega_0^{\text{Ge}} = 301\text{ cm}^{-1}$ and $\omega_0^{\text{Si}} = 520\text{ cm}^{-1}$ are the bulk Ge and Si Raman frequencies, respectively, and the linear coefficients are found to be $\alpha_{\text{Ge-Ge}}^{\text{GeSi}} = 19.4\text{ cm}^{-1}$ and $\alpha_{\text{Si-Si}}^{\text{GeSi}} = 67.9\text{ cm}^{-1}$.¹⁸ These dependencies have been quantitatively

TABLE II. Linear coefficients for the compositional dependence of Raman frequencies in binary and ternary Ge-Si-Sn alloys (cm^{-1}).

	Binary alloys	Ternary alloy
$\alpha_{\text{Ge-Ge}}^{\text{GeSi}}$	19.4 ^a	17.1 \pm 2.6
$\alpha_{\text{Ge-Ge}}^{\text{GeSn}}$	75.4 \pm 4.5 ^b	94.0 \pm 7.1
$\alpha_{\text{Si-Si}}^{\text{GeSi}}$	67.9 ^a	71.2 \pm 1.7
$\alpha_{\text{Si-Si}}^{\text{SiSn}}$	N/A	213 \pm 12

^aReference 18.

^bReference 30.

reproduced via first-principles calculations.²⁹ More recently,¹⁹ results for $\text{Ge}_{1-y}\text{Sn}_y$ alloys became available, and it was shown that, at least over the measured range of concentrations $y < 0.15$, the data can also be fitted with an expression of the form

$$\omega_{\text{Ge-Ge}}^{\text{GeSn}} = \omega_0^{\text{Ge}} - \alpha_{\text{Ge-Ge}}^{\text{GeSn}}y, \quad (3)$$

with $\alpha_{\text{Ge-Ge}}^{\text{GeSn}} = 68 \pm 5 \text{ cm}^{-1}$. More recent studies³⁰ that correct for epitaxial strain shifts give $\alpha_{\text{Ge-Ge}}^{\text{GeSn}} = 75.4 \pm 4.5 \text{ cm}^{-1}$.

In view of the results for binary compounds, we might expect the compositional dependence of the Ge-Ge and Si-Si modes in ternary $\text{Ge}_{1-x-y}\text{Si}_x\text{Sn}_y$ alloys to be linear in composition. We thus investigate expressions of the form

$$\omega_{\text{Ge-Ge}}^{\text{GeSiSn}}(x,y) = \omega_0^{\text{Ge}} - \alpha_{\text{Ge-Ge}}^{\text{GeSi}}x - \alpha_{\text{Ge-Ge}}^{\text{GeSn}}y, \quad (4a)$$

$$\omega_{\text{Si-Si}}^{\text{GeSiSn}}(x,y) = \omega_0^{\text{Si}} - \alpha_{\text{Si-Si}}^{\text{GeSi}}(1-x-y) - \alpha_{\text{Si-Si}}^{\text{SiSn}}y. \quad (4b)$$

Here, Eq. (4a) reduces to Eq. (2a) for $y=0$ and to Eq. (3) for $x=0$. Similarly, Eq. (4b) reduces to Eq. (2b) for $y=0$. For the case of vanishing Ge concentration ($x+y=1$), Eq. (4b) implies a linear dependence for the Si-Si mode frequency in the binary alloy $\text{Si}_{1-y}\text{Sn}_y$:

$$\omega_{\text{Si-Si}}^{\text{SiSn}} = \omega_0^{\text{Si}} - \alpha_{\text{Si-Si}}^{\text{SiSn}}y, \quad (5)$$

Preliminary Raman results from thin films of Si-rich $\text{Si}_{1-y}\text{Sn}_y$ alloys have been published recently.²⁷ In analogy with results from other group-IV alloys, these experiments show clear evidence for Si-Si and Si-Sn vibrations. A detailed compositional dependence of these modes was not reported in Ref. 27 due to the difficulties in determining composition and strain in very thin films.

We fitted our experimental data using the expressions in Eqs. (4a) and (4b), with $\alpha_{\text{Ge-Ge}}^{\text{GeSi}}$, $\alpha_{\text{Si-Si}}^{\text{GeSi}}$, $\alpha_{\text{Ge-Ge}}^{\text{GeSn}}$, and $\alpha_{\text{Si-Si}}^{\text{SiSn}}$ as adjustable parameters. The results from these two-dimensional fits are shown in Table II and Figs. 4 and 5. The fit coefficients $\alpha_{\text{Ge-Ge}}^{\text{GeSi}}$, $\alpha_{\text{Si-Si}}^{\text{GeSi}}$ are virtually identical to their counterparts in binary $\text{Ge}_{1-x}\text{Si}_x$ alloys, and the coefficient $\alpha_{\text{Ge-Ge}}^{\text{GeSn}}$ is also close to its value in binary $\text{Ge}_{1-y}\text{Sn}_y$ alloys. This suggests that the linear dependence proposed in Eqs. (4a) and (4b) extends over a much broader (x - y) range of compositions than actually measured, including the binary alloys as special cases. It is interesting to point out that Meléndez-Lira *et al.* used similar linear dependence expres-

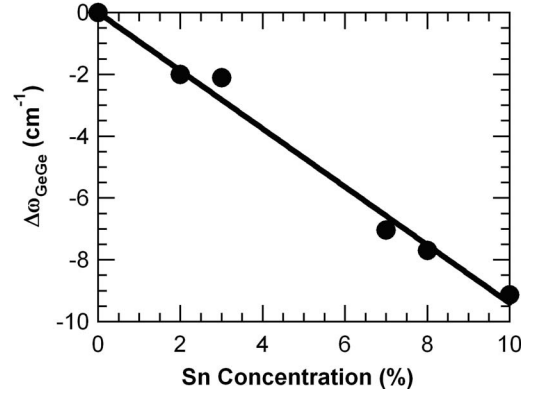


FIG. 4. The y dependence of the Ge-Ge mode frequency in $\text{Ge}_{1-x-y}\text{Si}_x\text{Sn}_y$ alloys. The data points are obtained by subtracting $\omega_0^{\text{Ge}} - \alpha_{\text{Ge-Ge}}^{\text{GeSi}}x$ from the strain-corrected Ge-Ge mode frequency ($\omega_0^{\text{Ge}} = 301 \text{ cm}^{-1}$, $\alpha_{\text{Ge-Ge}}^{\text{GeSi}} = 17.1 \text{ cm}^{-1}$). The line corresponds to the function $-\alpha_{\text{Ge-Ge}}^{\text{GeSn}}y$ ($\alpha_{\text{Ge-Ge}}^{\text{GeSn}} = 94 \text{ cm}^{-1}$). The coefficients $\alpha_{\text{Ge-Ge}}^{\text{GeSn}}$ and $\alpha_{\text{Ge-Ge}}^{\text{GeSi}}$ were obtained from a two-dimensional fit to the (x , y) dependence of the mode frequency according to Eq. (4a).

sions to analyze the compositional dependence of Raman modes in ternary $\text{Ge}_{1-x-y}\text{Si}_x\text{C}_y$ alloys. However, since the carbon concentrations were much lower, a two-dimensional fit was not possible, and the authors *assumed* that they could use the linear coefficients from $\text{Ge}_{1-x}\text{Si}_x$ alloys to extract the carbon dependence of the mode frequencies.

We have examined published experimental data for II-VI and III-V alloys to ascertain the generality of the above ideas. The compositional dependence of Raman mode frequencies in these systems is more complicated due to the sizable LO-TO splitting. This usually leads to quadratic terms in the compositional dependencies, which requires three additional coefficients when generalized to a two-dimensional semiconductor system. A possible way to avoid

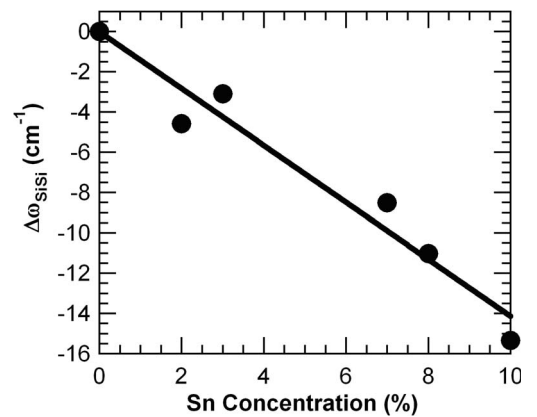


FIG. 5. The y dependence of the Si-Si mode frequency in $\text{Ge}_{1-x-y}\text{Si}_x\text{Sn}_y$ alloys. The data points are obtained by subtracting $\omega_0^{\text{Si}} - \alpha_{\text{Si-Si}}^{\text{GeSi}}(1-x)$ from the strain-corrected Si-Si mode frequency ($\omega_0^{\text{Si}} = 520 \text{ cm}^{-1}$, $\alpha_{\text{Si-Si}}^{\text{GeSi}} = 71.2 \text{ cm}^{-1}$). The line corresponds to the function $(\alpha_{\text{Si-Si}}^{\text{GeSi}} - \alpha_{\text{Si-Si}}^{\text{SiSn}})y$ ($\alpha_{\text{Si-Si}}^{\text{SiSn}} = 213 \text{ cm}^{-1}$). The coefficients $\alpha_{\text{Si-Si}}^{\text{GeSi}}$ and $\alpha_{\text{Si-Si}}^{\text{SiSn}}$ were obtained from a two-dimensional fit to the (x , y) dependence of the mode frequency according to Eq. (4b).

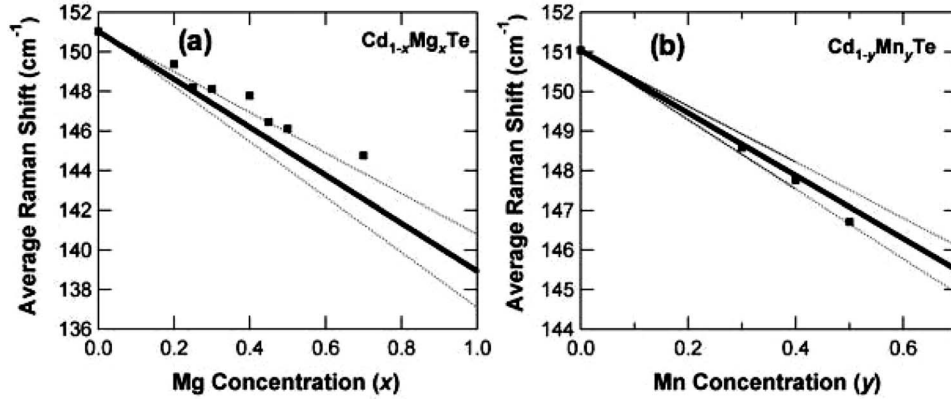


FIG. 6. The weighted average $\sqrt{(\omega_{LO}^2 + 2\omega_{TO}^2)}/3$ of the CdTe-like LO and TO Raman frequencies in (a) $\text{Cd}_{1-x}\text{Mg}_x\text{Te}$ and (b) $\text{Cd}_{1-y}\text{Mn}_y\text{Te}$ alloys (squares). The solid lines represent the x and y dependencies, respectively, obtained from a two-dimensional linear fit of the CdTe-like average frequency in $\text{Cd}_{1-x-y}\text{Mg}_x\text{Mn}_y\text{Te}$ quaternary alloys. The light dotted lines indicate the error in the bilinear fit. The original LO and TO Raman data are from Refs. 31 and 32.

these complications is to study the compositional dependence of the average mode frequency $\bar{\omega}_{A-B} = \sqrt{(\omega_{A-B}^{LO})^2 + 2(\omega_{A-B}^{TO})^2}/3$, which is independent of the ionic effective charges. Unfortunately, detailed Raman data for both the LO and TO modes as a function of composition are not always available due to the different selection rules for these modes, but in the few cases in which the analysis can be performed, we find that the average frequency is indeed linear in composition and can be expressed in terms of the compositional dependence of the corresponding average in the underlying pseudobinary alloys. As an example, we show in Fig. 6 results from Ramdas and co-workers^{31,32} for pseudoternary $\text{Cd}_{1-x-y}\text{Mg}_x\text{Mn}_y\text{Te}$ alloys and their related pseudobinaries. For the Mn dependence, the linear term obtained from the pseudoternary data provides an excellent fit of the corresponding pseudobinary $\text{Cd}_{1-y}\text{Mn}_y\text{Te}$ alloys, whereas for the Mg dependence, the discrepancy is within one standard deviation. This is similar to our findings for group-IV systems.

C. Scaling of linear coefficients for Si-Si and Ge-Ge modes in group-IV alloys

The compositional dependence of the $M-M$ Raman frequencies in $M_{1-x}N_x$ group-IV alloys can be understood by considering the formation of the alloy as a two-step process.^{3,33} In the first step, the atomic masses of a fraction x of M atoms are replaced with N -atom masses. All atoms remain at their original diamond-structure positions. This produces a frequency shift of the Raman-active modes akin to the confinement shifts observed in superlattices. An additional shift results from the bond deformations as the system relaxes to equilibrium when the imaginary M -type atoms with N -type masses are replaced by real N atoms. Thus we can write

$$\Delta\omega(x) = \Delta\omega^{\text{mass}}(x) + \Delta\omega^{\text{bond}}(x) \quad (6)$$

[strictly speaking, the additivity of the two steps applies to the shifts of the *squared* frequencies, but since the total shifts

are a small fraction of the bulk frequencies, a linearized version as in Eq. (6) is a good approximation]. The mass term can be easily modeled using the well-known bulk *ab initio* force constants, and it has been found to be proportional to the alloy fraction x .²⁰ The bond term can also be obtained from first principles using an interatomic potential expansion that includes third-order (anharmonic) derivatives of the total energy with respect to displacements from the diamond-structure positions.²⁹ Explicit calculations show that only terms that involve near neighbors are needed to obtain good agreement with experiment. Based on these ideas, Eq. (6) was written in Ref. 19 as

$$\begin{aligned} \Delta\omega_{M-M}(x) &= -A\omega_0^M x - B\omega_0^M \frac{\Delta R_{M-M}(x)}{R_0^M} \\ &= -A\omega_0^M x - B\omega_0^M (1 - a_{M-M}^{**}) \frac{\Delta a(x)}{a_0^M}, \end{aligned} \quad (7)$$

where the first term gives the mass contribution and the second term corresponds to the bond contribution. Here, ω_0^M is the Raman mode frequency of the elemental semiconductor M (i.e., the Raman frequency for $x=0$). The second term, first proposed by Carles *et al.*,³⁴ is the simplest possible expression consistent with the results of de Gironcoli.²⁹ Here, $\Delta R_{M-M}(x) = R_{M-M}(x) - R_0^M$, where $R_{M-M}(x)$ is the $M-M$ bond length in the alloy, and R_0^M is the $M-M$ bond length in the elemental semiconductor M . The change in bond length is related to $\Delta a(x) = a^{MN}(x) - a_0^M$, the change in cubic lattice constant, via the bond rigidity parameter a^{**} defined by Cai and Thorpe.³⁵ For group-IV alloys, it has been shown that $a^{**} = 0.6-0.7$, indicating a considerable degree of rigidity in the nearest-neighbor bonds.³⁵⁻³⁷ Since group-IV alloys follow Vegard's law quite closely, $\Delta a(x) = (a_0^N - a_0^M)x$. Therefore, the bond contribution should also be proportional to x , and this gives an overall compositional dependence that is linear in x , as found experimentally.

From *ab initio* supercell calculations, one obtains $A = 0.094$ (0.111) for the Si-Si (Ge-Ge) mode in $\text{Ge}_{1-x}\text{Si}_x$ alloys.²⁰ Combining this result with $a^{**} = 0.6$ and the experi-

mental compositional dependence of the Raman frequencies, one finds $B=2.45$ (2.60) for the Si-Si (Ge-Ge) modes. The similarity of the A and B parameters for both modes suggests that they are approximately mode and material independent, and this was explained in Ref. 19 by invoking the similarity of the phonon dispersion relations in group-IV elemental semiconductors. For example, it was argued that in the limit $x \rightarrow 1$ the mass perturbation in Eq. (6) should shift the Raman frequency to a value close to the strongest peak in the optical phonon density of states, which occurs at ω_{\max} ; $0.9\omega_0$ in Si, Ge, and α -Sn.³⁸ This yields $A=0.1$, in good agreement with the numerical simulations. Similarly, the simplest model for the parameter B is to assume that it has the same value as for a uniform volume deformation in the bulk,³⁴ so that $B=3\gamma$, where γ is the Gruneisen parameter for the Raman mode. The Gruneisen parameter for the zone-center optical mode in diamond-structure semiconductors is very close to unity, so that we predict $B \approx 3$, independent of mode and material. This is also close to the fit values.

A first test of the above ideas was carried out in Ref. 19 by using the A and B parameters for the Si-Si mode in $\text{Ge}_{1-x}\text{Si}_x$ alloys to predict the compositional dependence of the Ge-Ge mode in $\text{Ge}_{1-y}\text{Sn}_y$ alloys. The predicted value was found to be in very good agreement with the measured compositional dependence. Under the assumption of Vegard's law for the lattice constants, which is a very good approximation for our alloys, a generalization of the model of Eq. (7) to ternary alloys leads to an expression that corresponds to the sum of the compositional dependencies for the underlying binary alloys. Thus the experimental results reported here are consistent with this model. Moreover, since the parameter a^{**} —which, in principle, is bond and material dependent—turns out to be nearly the same for all bonds within a given $M_{1-x}N_x$ alloy³⁵ and very similar for all alloys involving Si, Ge, and Sn, as indicated above, Eq. (7) suggests that the linear coefficients in the compositional dependence of M - M mode frequencies should scale as

$$-\frac{\alpha_{M-M}^{MN}}{\omega_0^M} = A + C\varepsilon^{MN}, \quad (8)$$

where $\varepsilon^{MN} = (a_0^N - a_0^M)/a_0^M$, and A and C are “universal” constants. The normalized coefficients $-\alpha_{M-M}^{MN}/\omega_0^M$ are plotted in Fig. 7 against the mismatch parameter ε^{MN} , and it is seen that they are indeed approximately linear in this parameter. We have included in the figure a data point for the Si-Si mode in $\text{Si}_{1-y}\text{C}_y$ alloys as deduced from measurements in ternary $\text{Si}_{1-x-y}\text{Ge}_x\text{C}_y$ alloys.²⁰ Even though this system deviates from Vegard's law and the mass term for the Si-Si mode in $\text{Si}_{1-y}\text{C}_y$ alloys is not the same as in $\text{Ge}_{1-x}\text{Si}_x$ alloys [as implied by Eq. (8)], we see that the agreement with the overall linear dependence is quite satisfactory. By contrast, the Ge-Ge mode in $\text{Ge}_{1-y}\text{C}_y$, as deduced from the same measurements in $\text{Si}_{1-x-y}\text{Ge}_x\text{C}_y$ alloys, deviates substantially from the linear correlation in Fig. 7, and was not included in this figure. It should be noted, however, that there is a large uncertainty as to the experimental compositional dependence of this mode, since measurements in binary $\text{Ge}_{1-y}\text{C}_y$ appear to be in

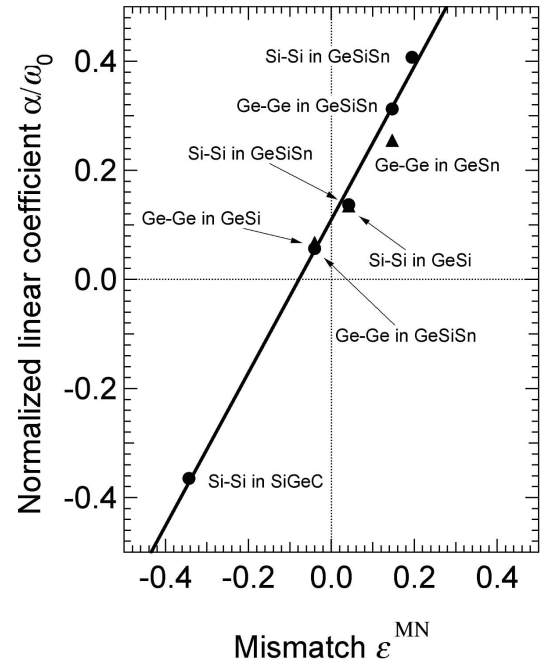


FIG. 7. Normalized linear coefficients for the compositional dependence of M - M Raman frequencies in group-IV $M_{1-x}N_x$ alloy systems as function of the lattice mismatch $\varepsilon^{MN} = (a_0^N - a_0^M)/a_0^M$ between the two elemental semiconductors M and N . The triangles correspond to data obtained from binary alloys, circles to data from ternary alloys. The solid line represents a linear fit as in Eq. (8), with $A=0.11$ and $C=1.40$.

complete disagreement with measurements in ternary alloys.³⁹ Thus more work is needed to ascertain to what extent carbon-containing alloys can be included in any exploration of scaling behaviors in the compositional dependence of group-IV alloy Raman frequencies. It is worth stressing here that the aforementioned scaling of phonon dispersion curves between α -Sn, Ge, and Si does not extend to diamond,³⁸ so that any vibrational mode involving C atoms should probably be excluded from the scaling analysis.

D. Compositional dependence of the Si-Ge mode

The compositional dependence of the Si-Ge Raman mode in $\text{Si}_x\text{Ge}_{1-x}$ alloys has been explained qualitatively in terms of the same ideas discussed in Sec. III C.³³ The Raman peak can be seen as derived from the zone-center optical mode in a hypothetical zinc blende SiGe structure, and therefore, the mass perturbation should lead to a maximum frequency at $x=0.5$. The bond perturbation corresponds to a compressive strain for $x > 0.5$ and a tensile strain for $x < 0.5$, and this reversal has been invoked to explain the steeper compositional dependence of the frequency for $x < 0.5$. In spite of this insight, a quantitative model equivalent to the one developed in Sec. III C has been elusive. The complexities become apparent when one compares the experimental Raman frequency at $x=0.5$, $\omega_{\text{Si-Ge}}(0.5) = 407 \text{ cm}^{-1}$ with the expected Raman frequency from a perfectly ordered zinc blende SiGe crystal, which, following the scaling of phonon

dispersion curves with the ionic plasma frequency, can be predicted to be $\omega_{zB}=420\text{ cm}^{-1}$. Therefore, even though the composition is the same, there is a downshift of 13 cm^{-1} in the alloy due to the randomization of the atomic distribution. For the Ge-Ge and Si-Si modes, on the other hand, one automatically obtains the ordered parent semiconductors in the limits $x\rightarrow 0$ and $x\rightarrow 1$. Not surprisingly, the compositional dependence of the Si-Ge mode frequency requires more complex expressions (terms up to x^4) than the simple linear dependencies found for the Ge-Ge and Si-Si modes.

The generalization of the compositional dependence of the Si-Ge mode to a two-dimensional compositional space introduces at least ten additional coefficients. Consequently, these parameters can only be determined with a much larger set of samples spanning the entire compositional space. Aside from these numerical considerations, the underlying physics is more complicated due to the similarity of the reduced Si-Ge and Si-Sn masses. In order to compare our experimental data with the simplest possible predictions in the spirit of the model used above for Si-Si and Ge-Ge modes, we consider two extreme limits: if we neglect the difference in the reduced masses, the quantity $\Delta\omega_{\text{Si-Ge}}=\omega_{\text{Si-Ge}}(x,y)-\omega_{\text{Si-Ge}}(x)$ should reflect the additional bond distortion contribution introduced by the Sn atoms. If we compute this using the model of Eq. (7) and averaging the values of the B parameters for the Si-Si and Ge-Ge modes, we obtain (using $a^{**}=0.6$) $\Delta\omega_{\text{Si-Ge}}=-70y$ (in cm^{-1}). In Fig. 8(a), we show this quantity computed by subtracting $\omega_{\text{Si-Ge}}(x)$ from the experimental data in Table I. The values of $\omega_{\text{Si-Ge}}(x)$ were computed from the proposed fourth-order polynomial expression in Ref. 18. A linear fit to the data (with a constant term to account for a possible error in the published Si-Ge mode frequencies) gives $\Delta\omega_{\text{Si-Ge}}=-109y$ (in cm^{-1}). This could be considered acceptable given the crudeness of the model. A somewhat better agreement can be obtained by taking the point of view that the mass difference between Ge and Sn is sufficient to confine the Si-Ge mode eigenvectors to Si-Ge bonds, so that the presence of a y fraction of Sn would add a mass and bond shift to the Si-Ge mode frequency in a $\text{Ge}_{1-x}\text{Si}_x$ alloy with $x'=x/(1-y)$. If we plot the quantity $\Delta\omega'_{\text{Si-Ge}}=\omega_{\text{Si-Ge}}(x,y)-\omega_{\text{Si-Ge}}(x')$ and fit it with a linear function of y [see Fig. 8(b)], we obtain $\Delta\omega'_{\text{Si-Ge}}=-112y$. Using an expression equivalent to Eq. (7), and averaging the values of the A and B parameters for the Si-Si and Ge-Ge modes, we now predict (again using $a^{**}=0.6$) $\Delta\omega'_{\text{Si-Ge}}=-110y$. Thus it appears that the model described in Eq. (7) can be used to understand the y dependence of the Si-Ge mode in, at least, a semiquantitative way.

IV. CONCLUSION

The analysis of the Raman spectra of $\text{Ge}_{1-x-y}\text{Si}_x\text{Sn}_y$ alloys presented here yields a comprehensive picture of Ge-Ge and Si-Si type vibrations in group-IV alloys made of Si, Ge, and Sn. The compositional dependence of these modes is found to be linear, and therefore, it appears that the ternary compositional dependence can be predicted from studies of binary alloys. The linear coefficients for the compositional dependence of Ge-Ge and Si-Si modes are found to follow a scal-

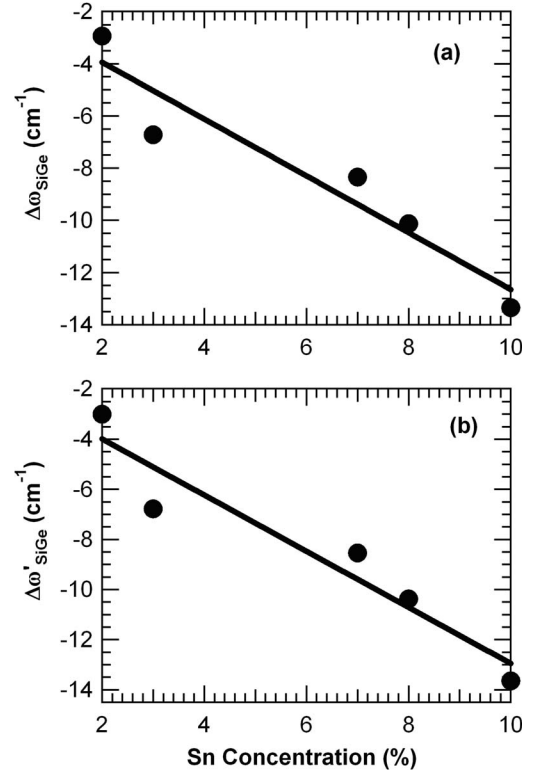


FIG. 8. The y dependence of the Si-Ge mode frequency in $\text{Ge}_{1-x-y}\text{Si}_x\text{Sn}_y$ alloys. (a) The data points are the difference between the strain-corrected Si-Ge mode frequency in the ternary alloy and the known frequency $\omega_{\text{Si-Ge}}^{\text{GeSi}}(x)$ of the same mode in $\text{Ge}_{1-x}\text{Si}_x$ alloys, as quoted in Ref. 18. The line represents a linear fit to the data. (b) The data points are the difference between the strain-corrected Si-Ge mode frequency in the ternary alloy and the frequency $\omega_{\text{Si-Ge}}^{\text{GeSi}}(x')$ of the same mode in $\text{Ge}_{1-x'}\text{Si}_{x'}$ alloys, where $x'=x/(1-y)$. The line represents a linear fit to the data. The motivation for these two alternative ways of displaying the results is discussed in the text.

ing behavior that can be traced back to the scaling of the phonon dispersion relations in Si, Ge, and α -Sn. It is worth noting that *ab initio* calculations have revealed a similarity of vibrational force constants for all tetrahedral semiconductors.¹⁶ Consequently, as suggested by our analysis of a II-VI alloy system, the compositional dependence of Raman modes in tetrahedral semiconductors should display scaling correlations similar to the ones discussed here.

It is important to point out that our studies have focused on mode frequencies, but the Raman spectra provide a wealth of additional information on the microscopic structure of the alloy systems. For example, a clear correlation between the width of the Raman spectra and the width of the bond length distribution function has been noted in Ref. 27. We believe that the combination of first-principles calculations and Raman spectroscopy can provide unique insights into the microscopic structure of semiconductor alloys that are impossible to obtain with any other experimental technique. Surprisingly, little progress has been made in *ab initio* simulations of the Raman spectra of semiconductor alloys since the pioneering work of de Gironcoli.²⁹

ACKNOWLEDGMENTS

This work was partially supported by the Air Force Office of Scientific Research under Grant No. FA9550-60-01-0442

(MURI program) and by Intel Corporation. We are particularly grateful to Anant K. Ramdas from Purdue University for several discussions and for kindly providing enlarged figures of his prior Raman work on alloy semiconductors.

- ¹L. Vegard, *Z. Phys.* **5**, 17 (1921).
- ²I. Vurgaftman, J. R. Meyer, and L. R. Ram-Mohan, *J. Appl. Phys.* **89**, 5815 (2001).
- ³J. Menéndez, in *Raman Scattering in Materials Science*, edited by W. H. Weber and R. Merlin (Springer, Berlin, 2000), Vol. 42, p. 55.
- ⁴V. Rakovics, A. L. Toth, B. Podor, C. Frigeri, J. Balazs, and Z. E. Horvath, *Mater. Sci. Eng., B* **91-92**, 83 (2002).
- ⁵G. A. Antypas, in *GaInAsP Alloy Semiconductors*, edited by T. P. Pearsall (Wiley, Chichester, 1982), p. 3.
- ⁶H. Law, R. Chin, K. Nakano, and R. Milano, *IEEE J. Quantum Electron.* **17**, 275 (1981).
- ⁷K. Godo, H. Makino, M. W. Cho, J. H. Chang, Y. Yamazaki, T. Yao, M. Y. Shen, and T. Goto, *Appl. Phys. Lett.* **79**, 4168 (2001).
- ⁸K. Shim, H. Rabitz, J.-H. Chang, and T. Yao, *J. Cryst. Growth* **214-215**, 350 (2000).
- ⁹D. Alexandropoulos and M. J. Adams, *IEE Proc.: Optoelectron.* **150**, 40 (2003).
- ¹⁰R. Gaska, A. Zukauskas, M. S. Shur, and M. A. Khan, *Proc. SPIE* **4776**, 82 (2002).
- ¹¹M. Ghali, J. Kossut, E. Janik, and W. Heiss, *Semicond. Sci. Technol.* **19**, 359 (2004).
- ¹²V. R. D'Costa, C. S. Cook, J. Menéndez, J. Tolle, J. Kouvetakis, and S. Zollner, *Solid State Commun.* **138**, 309 (2006).
- ¹³D. H. Jaw, Y. T. Cherng, and G. B. Stringfellow, *J. Appl. Phys.* **66**, 1965 (1989).
- ¹⁴E. Oh, R. G. Alonso, I. Miotkowski, and A. K. Ramdas, *Phys. Rev. B* **45**, 10934 (1992).
- ¹⁵O. K. Kim and W. G. Spitzer, *J. Appl. Phys.* **50**, 4362 (1979).
- ¹⁶P. Giannozzi, S. de Gironcoli, P. Pavone, and S. Baroni, *Phys. Rev. B* **43**, 7231 (1991).
- ¹⁷A. Ramam and S. J. Chua, *J. Appl. Phys.* **80**, 7157 (1996).
- ¹⁸H. K. Shin, D. J. Lockwood, and J.-M. Baribeau, *Solid State Commun.* **114**, 505 (2000).
- ¹⁹S. F. Li, M. R. Bauer, J. Menéndez, and J. Kouvetakis, *Appl. Phys. Lett.* **84**, 867 (2004).
- ²⁰M. Meléndez-Lira, J. Menéndez, W. Windl, O. F. Sankey, G. S. Spencer, S. Segó, R. B. Culbertson, A. E. Bair, and T. L. Alford, *Phys. Rev. B* **54**, 12866 (1997).
- ²¹J. Kouvetakis, J. Menéndez, and A. V. G. Chizmeshya, *Annu. Rev. Mater. Res.* **36**, 497 (2006).
- ²²A. V. G. Chizmeshya, M. R. Bauer, and J. Kouvetakis, *Chem. Mater.* **15**, 2511 (2003).
- ²³D. J. Lockwood and Z. R. Wasilewski, *Phys. Rev. B* **70**, 155202 (2004).
- ²⁴F. Cerdeira, C. J. Buchenauer, F. H. Pollak, and M. Cardona, *Phys. Rev. B* **5**, 580 (1972).
- ²⁵J. C. Tsang, P. M. Mooney, F. Dacol, and J. O. Chu, *J. Appl. Phys.* **75**, 8098 (1994).
- ²⁶M. Canonico (private communication).
- ²⁷J. Tolle, A. V. G. Chizmeshya, Y. Y. Fang, J. Kouvetakis, V. R. D'Costa, C. W. Hu, J. Menéndez, and I. S. T. Tsong, *Appl. Phys. Lett.* **89**, 231924 (2006).
- ²⁸D. L. Price, J. M. Rowe, and R. M. Nicklow, *Phys. Rev. B* **3**, 1268 (1971).
- ²⁹S. de Gironcoli, *Phys. Rev. B* **46**, 2412 (1992).
- ³⁰V. R. D'Costa, J. Tolle, C. D. Poweleit, J. Menéndez, and J. Kouvetakis (unpublished).
- ³¹S. Venugopalan, A. Petrou, R. R. Galazka, A. K. Ramdas, and S. Rodriguez, *Phys. Rev. B* **25**, 2681 (1982).
- ³²E. Oh, C. Parks, I. Miotkowski, M. D. Sciacca, A. J. Mayur, and A. K. Ramdas, *Phys. Rev. B* **48**, 15040 (1993).
- ³³J. Menéndez, A. Pinczuk, J. Bevk, and J. P. Mannaerts, *J. Vac. Sci. Technol. B* **6**, 1306 (1988).
- ³⁴R. Carles, G. Landa, and J. B. Renucci, *Solid State Commun.* **53**, 179 (1985).
- ³⁵Y. Cai and M. F. Thorpe, *Phys. Rev. B* **46**, 15872 (1992).
- ³⁶S. de Gironcoli, P. Giannozzi, and S. Baroni, *Phys. Rev. Lett.* **66**, 2116 (1991).
- ³⁷J. Shen, J. Zi, X. Xie, and P. Jiang, *Phys. Rev. B* **56**, 12084 (1997).
- ³⁸W. Weber, *Phys. Rev. B* **15**, 4789 (1977).
- ³⁹B.-K. Yang, W. H. Weber, and M. Krishnamurthy, in *Silicon-Germanium-Carbon Alloys: Growth, Properties, and Applications*, edited by S. T. Pantelides and S. Zollner (Taylor and Francis, New York, 2002), Vol. 15, p. 291.